The 4th IEEE International Conference on E-Health and Bioengineering - EHB 2013
Grigore T. Popa University of Medicine and Pharmacy, Iaşi, Romania, November 21-23, 2013

A novel approach for computing pressure drop in healthy and mildly stenosed arteries

Olivia Florea
Transilvania University of Brasov
Faculty of Mathematics and Computer Sciences
Brasov, Romania
olivia.florea@unitbv.ro

***Abstract*—Blood pressure levels are highest in the arterial systemic circulation and play a crucial role in the diagnosis of local pathologies (e.g. stenoses). Under certain physiological conditions, pressure drop over healthy and mildly stenosed arteries can become important, contributing significantly to the overall pressure drop in an arterial tree. We propose a fully analytical approach for estimating the pressure drop in such arteries, using the power-law fluid to model blood flow. The studied model of the stenosis is considered axisymmetric, and having a bell shape. To validate the method, we considered three coronary epicardial vessels with different flow rate values and compared results against a previously validated model. The results showed that the proposed method is able to correctly estimate the pressure drop for healthy and mildly stenosed arteries with a stenosis grade of up to 18% (for large arteries) and 41% (for small arteries).**

***Keywords*—pressure drop, analytical model, artery, stenosis, blood.**

I. INTRODUCTION

The cardiovascular system is composed of two subsystems: the systemic circulation and the pulmonary circulation. Both contain an arterial part, which supplies blood from the heart to the tissues and a venous part which transports the blood back to the heart. Blood pressure levels are considerably higher in the arterial part than in the venous part, and at least three times higher in the systemic circulation than in the pulmonary circulation [1]. Hence, most pathologic conditions related to blood pressure levels have been reported for the systemic arterial circulation [2].

Sudden pressure changes in the large systemic arteries appear as a result of constrictions (stenoses, coarctation) or enlargements (aneurysms) of the vessels, and play a crucial role in the diagnosis of these pathologies [3]. The majority of research activities reported in literature for arterial constrictions focused on severe cases where the radius is reduced by 50% or more.

Young et al. showed that a quadratic relationship can be established between pressure drop and flow rate, and determined a set of empirical parameters based on a curve fit to experimental data [4].

Huo et al. introduced an analytically derived pressure drop model for coronary stenoses which was validated against in vivo and in vitro experiments [5]. Different pressure drop models were also proposed for the aortic valve [6] or for aortic coarctations [7].

To study the hemodynamics of an arterial tree, these analytical or empirical models were often coupled to blood flow models: entire systemic circulation [8], coronary circulation [9], proximal aorta [10-13]. High performance computing techniques are usually employed for these blood flow models to accelerate the execution time [14], [15].

Average pressure drop in large, healthy systemic arteries is considered to be negligible. However, under certain physiological conditions, like intense exercise, pressure drop over healthy segments can not be entirely discarded [16]. Although, as a standalone component, pressure drop in healthy vessels does not lead to pathologic symptoms, it can contribute substantially to the overall pressure drop in a pathologic arterial tree.

The goal of this paper is to introduce a novel approach for computing pressure drop in healthy and mildly stenosed arteries. The method is fully analytical and uses the arterial geometry and the flow rate as input parameters. It can be used together with the above mentioned pressure drop models to compute the pressure drop for an entire arterial tree.

The paper is organized as follows. In section II we describe the methodology for computing pressure drop in the arterial systemic circulation. Section III presents detailed results for coronary arteries, while section IV provides a brief discussion and draws the conclusions.

II. METHODS

To introduce the proposed method, we consider an artery with the radius R and a total length L. The pressure drop over the entire length of the artery is Δp and the flow rate through the artery is q. The model is derived under the assumption that blood flow through the artery is uniform and unidirectional. The axial momentum of the blood satisfies the relation, [17], [18]:

$$-\frac{dp}{dx}+\frac{1}{r}\frac{d(r\sigma)}{dr}=0, \quad (1)$$

By integrating this equation with respect to r and substituting dp with Δp, we obtain:

$$\sigma=\frac{r}{R}\sigma_{wall}, \quad (2)$$

978-1-4799-2373-1/13/$31.00 ©2013 IEEE

where σ_{wall} represents the wall shear stress and is given by:

$$\sigma_{wall} = \frac{\Delta p \cdot R}{2L} \tag{3}$$

The power law or the Ostwald de Waele relation is a type of generalization of the Newtonian fluid which has the shear stress:

$$\sigma = K\left(\frac{\partial u}{\partial r}\right)^n, \tag{4}$$

where: K is the density index, obtained from the equation $\mu = K \cdot \left(\frac{\partial u}{\partial r}\right)^{n-1}$, μ is the effective viscosity as a function of the shear rate; $\partial u / \partial r$ is the velocity gradient, which is perpendicular on the shear plane; n is the index which represents the behavior of the flow.

From (2) and (4) we obtain:

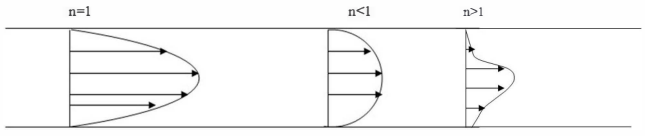

Fig. 1. Velocity profiles for different values of n.

$$K\left(\frac{\partial u}{\partial r}\right)^n = \frac{r}{R}\sigma_{wall} \Rightarrow \left(\frac{\partial u}{\partial r}\right)^n = \frac{r}{KR}\sigma_{wall} \Leftrightarrow \frac{\partial u}{\partial r} = \frac{r^{\frac{1}{n}}}{(KR)^{\frac{1}{n}}}\sigma_{wall}^{\frac{1}{n}} \tag{5}$$

By integrating this equation with respect to $r \in [r, R]$ we obtain:

$$u = \left(\frac{\sigma_{wall}}{KR}\right)^{\frac{1}{n}} \frac{r^{\frac{1}{n}+1}}{\frac{1}{n}+1}\Bigg|_r^R \Leftrightarrow u = \left(\frac{\sigma_{wall}}{KR}\right)^{\frac{1}{n}} \frac{R^{\frac{1}{n}+1} - r^{\frac{1}{n}+1}}{\frac{1}{n}+1} \tag{6}$$

For different values of n, the ratio between the axial velocity and the radius is different, hence for Newtonian blood flow (Poiseuille) n = 1, the pressure gradient is zero (dp/dx = 0). For shear thinning n < 1, the flow profile is flattened in the middle and then decreases rapidly towards the wall, and the pressure gradient is positive: dp/dx > 0. The case of n > 1 is encountered for very viscous fluids, for which the pressure gradient is negative dp/dx < 0. The velocity profiles for various values of n are displayed in fig. 1, [19].

The flow rate through the artery is given by:

$$Q = \int_0^R u \cdot 2\pi r dr = \pi \frac{\sigma_{wall}^{\frac{1}{n}}}{K^{\frac{1}{n}}} \cdot \frac{R^3}{\frac{1}{n}+3}. \tag{7}$$

Taking into account equation (3), we obtain:

$$Q = \frac{\pi R^3}{\frac{1}{n}+3}\left(\frac{\Delta p \cdot R}{2LK}\right)^{\frac{1}{n}}. \tag{8}$$

As function of the axial velocity, the flow rate can be expressed as:

$$Q = \int_0^R u(r) 2\pi r dr = u\pi r^2\Big|_0^R - \int_0^R \frac{du}{dr}\pi r^2 dr. \tag{9}$$

When the axial velocity is zero on the boundary (without boundary slip conditions) we obtain:

$$Q = -\int_0^R \frac{du}{dr}\pi r^2 dr. \tag{10}$$

Using equation (2), the radius can be expressed as a function of the wall stress:

$$r = \frac{R\sigma}{\sigma_{wall}}; r = r(\sigma) \Leftrightarrow \frac{du}{dr} = \frac{du}{d\sigma}. \tag{11}$$

By applying this change of variable in the last integral we obtain:

$$r = 0 \Rightarrow \sigma = 0; r = R \Rightarrow \sigma = \sigma_{wall} \Rightarrow dr = \frac{R}{\sigma_{wall}} d\sigma$$

leading to:

$$Q = -\pi\left(\frac{R}{\sigma_{wall}}\right)^3 \int_0^{\sigma_{wall}} \frac{du}{dr(\sigma)}\sigma^2 d\sigma, \tag{12}$$

where $\frac{du}{dr(\sigma)} = \dot{\gamma}(\sigma)$ represents the deformation rate. Because the deformation rate is a function of the stress, the material properties are described. If we compute the derivative of the flow rate with respect to the wall stress σ_{wall}, we obtain:

$$\frac{dQ}{d\sigma_{wall}} = \frac{3\pi R^3}{\sigma_{wall}^4}\int_0^{\sigma_{wall}} \dot{\gamma}(\sigma)\cdot\sigma^2 d\sigma - \frac{\pi R^3}{\sigma_{wall}^3}\cdot\dot{\gamma}(\sigma_{wall})\cdot\sigma_{wall}^2. \tag{13}$$

From (12) we obtain:

$$\frac{dQ}{d\sigma_{wall}} = \frac{3\pi R^3}{\sigma_{wall}^4}\cdot\left(-\frac{Q\cdot\sigma_{wall}^3}{\pi R^3}\right) - \frac{\pi R^3}{\sigma_{wall}}\cdot\dot{\gamma}(\sigma_{wall}) = -\frac{3Q}{\sigma_{wall}} - \frac{\pi R^3}{\sigma_{wall}}\cdot\dot{\gamma}(\sigma_{wall}) \tag{14}$$

and, hence:

$$\dot{\gamma}(\sigma_{wall}) = -\frac{1}{\pi R^3}\left(3Q + \sigma_{wall}\frac{dQ}{d\sigma_{wall}}\right) = -\frac{1}{\pi R^3}\left(3Q + \frac{\Delta p\cdot R}{2L}\frac{dQ}{d\sigma_{wall}}\right) \tag{15}$$

Since

$$\sigma_{wall} = \frac{\Delta p\cdot R}{2L} \Leftrightarrow \Delta p = \frac{2L\sigma_{wall}}{R}$$

equation (15) becomes:

$$\dot{\gamma}(\sigma_{wall}) = -\frac{1}{\pi R^3}Q\left(3 + \frac{\Delta p\cdot R}{2L}\cdot\frac{\frac{dQ}{d\sigma_{wall}}}{Q}\right) = -\frac{1}{\pi R^3}Q\frac{\Delta p\cdot R}{2L}\left(\frac{3}{\frac{\Delta p\cdot R}{2L}} + \frac{\frac{dQ}{d\sigma_{wall}}}{\frac{Q}{\frac{\Delta p\cdot R}{2L}}}\right) = \tag{16}$$

$$= -\frac{1}{\pi R^3}Q\frac{\Delta p\cdot R}{2L}\left(\frac{3}{\sigma_{wall}} + \frac{d(\ln Q)}{\frac{d(\Delta p)}{\Delta p}}\right) = -\frac{1}{\pi R^3}Q\frac{\Delta p\cdot R}{2L}\left(\frac{3}{\sigma_{wall}} + \frac{d(\ln Q)}{d(\ln \Delta p)}\right)$$

The following aspects are emphasized, [20]:

- for a Newtonian flow we obtain: $\frac{d(\ln Q)}{d(\ln \Delta p)} = 1$
- for a shear thinning (pseudo-plastics) with n = 1/4 we obtain $\frac{d(\ln Q)}{d(\ln \Delta p)} = 4$
- for any type of fluid, the deformation rate can be computed with the rheological law

$$\mu_{wall} = \frac{\sigma_{\text{rheologic}}}{\dot{\gamma}(\sigma_{\text{rheologic}})} = \frac{\Delta p\cdot R}{2L\cdot\dot{\gamma}(\sigma_{\text{rheologic}})} \tag{17}$$

To study the pressure over mildly stenosed arteries we consider the following stenosis geometry [21]:

$$R(x) = R_0 - \frac{R_s}{2}\left[1 - cos2\pi\frac{x - L_m - \frac{L_s}{2}}{L_s}\right] \tag{18}$$

R_s is the maximum radius reduction of the stenosis, R_0 is the healthy radius, L_s is the length of the artery, while $L_m = L_s/2$.

By integrating the equation of the axial momentum (1) and taking into account that, in regular conditions, if σ is finite then $r = 0$, we obtain:

$$\sigma = \frac{r}{2}\frac{dp}{dx} \tag{19}$$

The surface friction is computed as follows:

$$\sigma_{wall} = \frac{R}{2}\frac{dp}{dx}, R = R(x) \tag{20}$$

In equation (12) we replace du/dr with the form obtained in equation (6):

$$Q = \frac{\pi R^3}{\sigma_{wall}^3}\int_0^{\sigma_{wall}} \sigma^2 \cdot \frac{r^{\frac{1}{n}}}{(KR)^{\frac{1}{n}}}\sigma_{wall}^{\frac{1}{n}} d\sigma. \tag{21}$$

Therefore, from equation (11) we obtain:

$$Q = \frac{\pi R^3}{\sigma_{wall}^3 \cdot K^{\frac{1}{n}}}\int_0^{\sigma_{wall}} \sigma^{2+\frac{1}{n}} d\sigma = \frac{\pi R^3}{\sigma_{wall}^3 \cdot K^{\frac{1}{n}}}\int_0^{\sigma_{wall}} \frac{\sigma_{wall}^{3+\frac{1}{n}}}{3+\frac{1}{n}} d\sigma = \frac{n\pi r^3}{3n+1}\left(\frac{\sigma_{wall}}{K}\right)^{\frac{1}{n}} \tag{22}$$

which leads to:

$$Q^n = \left(\frac{n\pi R^3}{3n+1}\right)^n \cdot \frac{1}{K} \cdot \left(\frac{R}{2}\frac{dp}{dx}\right). \tag{23}$$

Hence, the following equation is obtained:

$$\frac{dp}{dx} = \frac{2K}{R}\left(\frac{Q(3n+1)}{n\pi R^3}\right)^n \tag{24}$$

By integrating this equation along the length of the artery, and using the boundary conditions: $x = 0$, $p = p_1$, $x = L$, $p = p_2$, we obtain the final expression for the drop pressure:

$$\Delta p = 2K\left(\frac{Q(3n+1)}{n\pi}\right)^n \int_0^L \frac{dx}{R^{3n+1}} = \tag{25}$$

$$= 2K\left(\frac{Q(3n+1)}{n\pi}\right)^n \int_0^L \frac{dx}{R_0 - \frac{R_0 \cdot p}{200}\left[1 - \cos 2\pi \frac{x - L_m - \frac{L_s}{2}}{L_s}\right]}$$

III. RESULTS

The methodology described in the previous section was used to compute the pressure drop in different arterial configurations. We focus on large arteries, which resemble the epicardial coronary arteries (since blood in the large arteries behaves like a Newtonian fluid n = 1). Hence, we consider three different vessels with healthy radiuses of R_0 = 0.1 cm, R_0 = 0.15 cm, and R_0 = 0.2 cm. Different stenosis grades are considered, in the interval between 10% and 50%. The length of the stenosis is set to L_s = 4.0 cm, the dynamic viscosity is set to 0.04 g/(cm·s).

As mentioned in the introduction, pressure drop over healthy or mildly stenosed arteries can become significant under certain physiological conditions (e.g. increased flow rate) [22]. To estimate the flow rate at exercise, we first compute the flow rate at rest, based on the formula in [23]:

$$q = 1.43 \cdot d^{2.55} \tag{26}$$

where d is the diameter of the vessel.

Next, considering that the ratio of exercise to rest flow rate is 4.4 [24], the following flow rate values are obtained: 0.8249 ml/s, 2.3198 ml/s, and 4.8311 ml/s for the vessels with radiuses of 0.1 cm, 0.15 cm, and respectively 0.2 cm.

Table I displays the pressure drop values obtained for the different arterial configurations. To determine the maximum stenosis grade for which the proposed method can be applied, we compared the results against the values obtained with the model validated in [5].

TABLE I
PRESSURE DROP RESULTS FOR DIFFERENT ARTERIAL CONFIGURATIONS

R_0 [cm]	% Sten.	ΔP eq. (25) [g/(cm·s^2)]	ΔP model [5] [g/(cm·s^2)]
0.10	0	3360.9	-
	10	4183.9	4203.8
	20	5449.3	5563.4
	30	7528.4	7919.7
	40	11249.2	12389
	50	18715.3	21962
0.15	0	1867.0	-
	10	2324.2	2355.2
	20	3027.1	3205.9
	30	4182.0	4793.9
	40	6248.9	8033.8
	50	10396.4	15478.7
0.20	0	1230.2	-
	10	1531.5	1574.1
	20	1994.7	2240.0
	30	2755.7	3595.8
	40	4117.6	6568.6
	50	6850.5	13829.7

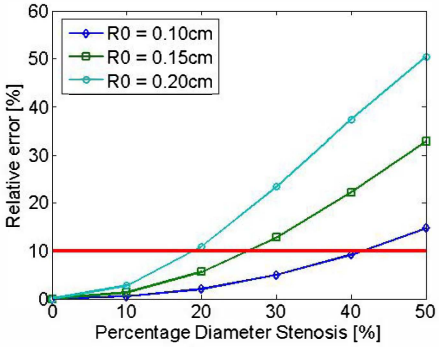

Fig. 2. Relative pressure drop differences between the model in (25) and the model in [5].

The results in Table I show that pressure drop values increase with more severe stenoses, both for the results obtained with (25) and with the model in [5]. Furthermore, pressure drop values are higher for smaller radiuses, confirming the fact that the larger an artery the smaller the pressure drop.

One can see that when the stenosis grade is small, the difference between our approach and the model in [5] is small. The difference increases for more severe stenosis. Moreover, differences between the results obtained with the two models are more significant for larger radiuses.

To correctly quantify the pressure drop differences obtained between the two models, we display in fig. 2 the relative differences for different radius values and different stenosis severities. The results emphasize the fact that the differences are smaller for smaller radiuses. We considered an error of 10% to be the threshold tolerance value (marked with a red line), and hence we can conclude that:

- when R_0 = 0.20 cm, results obtained with (25) are reliable for stenosis grades of up to 18%;
- when R_0 = 0.15 cm, results obtained with (25) are reliable for stenosis grades of up to 25%;
- when R_0 = 0.10 cm, results obtained with (25) are reliable for stenosis grades of up to 41%.

IV. Discussion and Conclusions

We introduced a fully analytical method for computing pressure drop in healthy and mildly stenosed arteries.

To validate the method, we considered three coronary epicardial vessels of different sizes, with different stenosis severities ranging from 10% to 50%. Moreover, since pressure drop over coronary vessels under hyperemic conditions plays a crucial role for the diagnosis of coronary stenoses [25], we analyzed the results for increased flow rates corresponding to the exercise state of patients. The results obtained herein were compared against the pressure drop results obtained with a model previously validated *in vitro* and *in vivo* [5]. Thus, as can be seen in fig. 2, the proposed method is able to correctly estimate the pressure drop both for healthy vessels and for mildly stenosed vessels. The stenosis grade up to which the results are reliable depends on the radius of the vessels.

The main difference between the model in (25) and the model in [5] is that we did not taken into account the turbulent energy losses which occur in the distal part of the stenosis. This aspect is responsible for the differences observed in Table I and will be taken into consideration for future research activities, to improve the proposed method.

Finally, the study has a series of limitations. First of all, we did not model the fact that the flow rate decreases in the presence of stenoses. Whereas this aspect is negligible for mild stenosis (with a grade smaller or equal to 30%) it can become significant for intermediate or severe stenoses (with a grade higher than 30%). Thus, the relative errors obtained for stenoses with grades equal to or higher than 30% are smaller than the values in Table I. Secondly, the pressure drop model introduced in [5], was only validated for stenoses with a grade higher than 40%.

Acknowledgment

This work is partially supported by the program Partnerships in Priority Domains (PN II), financed by ANCS, CNDI - UEFISCDI, under the project nr. 130/2012.

References

[1]. A. Nordergraaf, *Circulatory System Dynamics*, Academic Press, San Diego, USA, 1978.

[2]. D. A. Steinman and C. A. Taylor, "Flow Imaging and Computing: Large Artery Hemodynamics", *Annals of Biomedical Engineering*, vol. 33, 2005, pp. 1704–1709.

[3]. D. Ku, "Blood Flow In Arteries", *Annu. Rev. Fluid Mech.* 1997, vol. 29, pp. 399–434.

[4]. D. Young and F. Tsai, "Flow Characteristics in Models of Arterial Stenoses-i. Steady Flow", *Journal of Biomechanics*, vol. 6, 1973, pp. 395–410.

[5]. Y. Huo, M. Svendsen, J. S. Choy, Z. D. Zhang and G. S. Kassab, "A Validated Predictive Model of Coronary Fractional Flow Reserve", *Journal of the Royal Society Interface*, vol. 9, pp. 1325–38, 2012.

[6]. D. Garcia, P. Pibarot and L.G. Duranda, "Analytical Modeling of the Instantaneous Pressure Gradient across the Aortic Valve", *Journal of Biomechanics*, vol. 38, 2005, pp. 1303–1311.

[7]. Z. Keshavarz-Motamed, J. Garcia, P. Pibarot, E. Larose and L. Kadem, "Modeling the Impact of Concomitant Aortic Stenosis and Coarctation of the Aorta on Left Ventricular Workload", *Journal of Biomechanics*, vol. 44, 2011, pp. 2817–2825.

[8]. N. Stergiopulos, D. Young and T. Rogge, "Computer Simulation of Arterial Flow with Applications to Arterial and Aortic Stenosis", *Journal of Biomechanics*, vol. 25, 1992, pp. 1477–1488.

[9]. L.M. Itu, P. Sharma, V. Mihalef, A. Kamen, C. Suciu and D. Comaniciu, "A Patient-specific Reduced-order Model for Coronary Circulation", *Proc. of the IEEE Inter. Symp. On Biomedical Imaging - ISBI*, Barcelona, Spain, May 2012, pp. 832–835.

[10]. L. M. Itu, P. Sharma, M. A. Gulsun, V. Mihalef, A. Kamen, and A. Greiser, "Determination of Time-varying Pressure Field from Phase Contrast MRI Data", *Journal of Cardiovascular Magnetic Resonance*, vol. 14, Suppl. 1, 2012, pp. 36.

[11]. L.M. Itu, P. Sharma, K. Ralovich, V. Mihalef, R. Ionasec, A. Everett, R. Ringel, A. Kamen and D. Comaniciu, "Non-Invasive Hemodynamic Assessment of Aortic Coarctation: Validation with In Vivo Measurements", *Annals of Biomedical Engineering*, vol. 41, No. 4, 2013, pp. 669–681.

[12]. C. Niță, L. M. Itu, and C. Suciu, "GPU Accelerated Fluid Flow Computations using the Lattice Boltzmann Method", *Bulletin of the Transilvania University of Brasov - Series I*, vol. 55, 2013, pp. 67–74.

[13]. C. Niță, L. M. Itu, and C. Suciu, "GPU Accelerated Blood Flow Computation using the Lattice Boltzmann Method", *Proc. of the 17th IEEE High Performance Extreme Computing Conference*, Waltham, MA, USA, Sept. 2013.

[14]. L. M. Itu, C. Suciu, F. Moldoveanu, and A. Postelnicu, "GPU Optimized Computation of Stencil Based Algorithms", *Proc. of the 10th RoEduNet Inter. Conf.*, Iași, Romania, June 2011, pp. 1-4.

[15]. L. M. Itu, C. Suciu, F. Moldoveanu, and A. Postelnicu, "GPU Accelerated Simulation of Elliptic Partial Differential Equations", *Proc. of the 6th IEEE Inter. Conf. on Intelligent Data Acquisition and Advanced Computing Systems: Technology and Applications*, Prague, Czech Republic, Sept. 2011, pp. 238-242.

[16]. L. Grinberg and G. E. Karniadakis, G. E. "Outflow Boundary Conditions for Arterial Networks with Multiple Outlets", *Annals of Biomedical Engineering*, vol. 36, 2008, pp. 1496–1514.

[17]. J.C. Misra and G.C. Shit, "Blood flow through arteries in a pathological state: A theoretical study", *Int. J. of Engineering Science*, vol. 44, 2006, pp. 662-671

[18]. S. Singh and R.R. Shah, " A numerical model for the effect of stenosis shape on blood flow through an artery using power-law fluid", *Advances in Applied Science Research*, vol. 1, 2010, pp. 66-73.

[19]. R. Karch, F. Neumann, M. Neumann and W. Schreiner, " A three-dimensional mode for arterial tree representation, generated by constrained constructive optimization", *Computer in Biology and Medicine,* vol. 29, 1999, pp. 19-38.

[20]. E. J. Hinch, *Perturbation Methods*, Cambridge University Press, 1991

[21]. D. Bessems, *On the Propagation of Pressure and Flow Waves through the Patient-Specific Arterial System*, Ph.D. Thesis, TU Eindhoven, Netherlands, 2007.

[22]. C.S.N. Azwadi and M. Salehi, "Prediction of flow characteristics in stenosis artery using CIP scheme", *Int. Journal of Mechanical and Materials Engineering,* vol. 7, 2012, pp. 101-106.

[23]. A.van der Giessen, H. Groen, P.A. Doriot, P. de Feyter, A. van der Steen, F.van de Vosse, J. Wentzel and F. Gijsen, "The influence of boundary conditions on wall shear stress distribution in patient specific coronary trees", *Journal ofBiomechanics* , vol.44, 2011, pp. 1089–1095.

[24]. R. F. Wilson, K. Wyche, B. V. Christensen, S. Zimmer and D. D. Laxson, "Effects of Adenosine on Human Coronary Arterial Circulation", *Circulation*, vol. 82, 1990, pp. 1595–1606.

[25]. N. H. Pijls, B. De Bruyne, *Coronary Pressure*, Kluwer Academic Publishing, London, UK, 2000.